Electronic Supplementary Material (ESI) for Dalton Transactions.

Supporting Information

Enantiomeric pairs of copper(II) complexes with tridentate Schiff bases derived from *R*- and *S*-methionine: the role of decorating organic groups of the ligand in crystal packing and biological activity

Catalin Maxim[a], Cristian D. Ene*[a,b], Ioana Nicolau[c], Lavinia L. Ruta[c], Ileana C. Farcasanu*[c]

[a] Department of Inorganic Chemistry, Faculty of Chemistry, University of Bucharest, Str. Dumbrava Rosie 23, 020464-Bucharest, Romania.

[b] "Ilie Murgulescu" Institute of Physical Chemistry of the Romanian Academy, Coordination and Supramolecular Chemistry Laboratory, Splaiul Independentei 202, 060021-Bucharest, Romania.

[c] Department of Organic Chemistry, Biochemistry and Catalysis, Faculty of Chemistry, University of Bucharest, Sos. Panduri 90-92, 050663-Bucharest, Romania.

*Corresponding authors: Cristian D. Ene (cene@icf.ro), Ileana C. Farcasanu (ileana.farcasanu@chimie.unibuc.ro)

Table S1. Selected bond lengths (Å) and angles (º) for compounds **1-*R*·H$_2$O**, **1-*R***, **1-*S***, **2-*R***, and **2-*S***.

Compound	Distances (Å)		Angles (º)			
1-*R*·H$_2$O	Cu1-N1	1.938(3)	N1-Cu1-O1W	100.55(12)	O2-Cu2-O5	96.51(10)
	Cu1-O1^{i}	2.698	N1-Cu1-O2	81.24(11)	O2-Cu2-O2	87.78(12)
	Cu1-O1W	2.390(3)	N1-Cu1-O5	162.80(12)	O6-Cu2-N2	93.55(13)
	Cu1-O2	2.013(2)	O2-Cu1-O1W	83.40(10)	O6-Cu2-O5	170.53(11)
	Cu1-O3	1.907(3)	O2-Cu1-O3	172.02(11)		
	Cu1-O5^{i}	2.068(3)	O2-Cu1-O5	93.24(10)		
	Cu2-N2	1.915(3)	O3-Cu1-N1	93.20(12)		
	Cu2-O1	2.797	O3-Cu1-O1W	92.06(11)		
	Cu2-O2	1.971(3)	O3-Cu1-O5^{i}	93.69(10)		
	Cu2-O4^{i}	2.551	O5^{i}-Cu1-O1W	94.93(11)		
	Cu2-O5	2.057(3)	N2-Cu2-O2	173.99(12)		
	Cu2-O6	1.887(3)	N2-Cu2-O5	83.05(12)		
1-*R*	Cu1-N1	1.904(8)	N1-Cu1-O2	82.1(3)	O2-Cu2-O6	87.5(3)
	Cu1-O1^{ii}	2.522	N1-Cu1-O3	93.9(3)	O5-Cu2-O6	168.4(2)
	Cu1-O2	2.005(5)	N1-Cu1-O5	169.0(3)		
	Cu1-O3	1.881(6)	O2-Cu1-O3	163.9(3)		
	Cu1-O5^{ii}	1.990(6)	O2-Cu1-O5	95.6(2)		
	Cu2-N2	1.903(7)	O3-Cu1-O5	91.1(3)		
	Cu2-O2	1.973(6)	N2-Cu2-O2	175.7(3)		
	Cu2-O4^{ii}	2.523	N2-Cu2-O5	82.3(3)		
	Cu2-O5	2.028(6)	N2-Cu2-O6	94.0(3)		
	Cu2-O6	1.877(6)	O2-Cu2-O5	97.0(2)		
1-*S*	Cu1-N1	1.925(4)	N1-Cu1-O2	81.50(13)	O2-Cu2-O6	87.72(14)
	Cu1-O1^{ii}	2.523	N1-Cu1-O3	94.31(15)	O5-Cu2-O6	168.59(13)
	Cu1-O2	2.012(3)	N1-Cu1-O5	168.70(15)		
	Cu1-O3	1.890(3)	O2-Cu1-O3	164.30(15)		
	Cu1-O5^{ii}	1.998(3)	O2-Cu1-O5	95.71(12)		
	Cu2-N2	1.922(4)	O3-Cu1-O5	91.17(13)		
	Cu2-O2	1.974(3)	N2-Cu2-O2	175.76(15)		
	Cu2-O4^{ii}	2.515	N2-Cu2-O5	82.3(5)		
	Cu2-O5	2.028(3)	N2-Cu2-O6	93.89(15)		
	Cu2-O6	1.889(3)	O2-Cu2-O5	96.85(12)		
2-*R*	Cu1-N1	1.949(5)	N1-Cu1-O1^{iv}	161.68(16)	O2-Cu1-O3	175.42(18)
	Cu1-O1^{iv}	2.022(4)	N1-Cu1-O2	83.20(15)	O2-Cu1-O4^{iii}	85.8(16)
	Cu1-O2	1.950(4)	N1-Cu1-O3	94.33(17)	O3-Cu1-O4	98.66(15)
	Cu1-O2^{iv}	2.593	N1-Cu1-O4	104.72(17)		
	Cu1-O3	1.897(4)	O1^{iv}-Cu1-O2	87.55(15)		
	Cu1-O4^{iii}	2.316(4)	O1^{iv}-Cu1-O4^{iii}	90.27(15)		
2-*S*	Cu1-N1	1.957(5)	N1-Cu1-O1^{iv}	161.8(2)	O3-Cu1-O4	175.4(3)
	Cu1-O1^{iv}	2.033(5)	N1-Cu1-O2	84.1(5)	O2-Cu1-O4^{iii}	85.7(2)
	Cu1-O2	1.954(5)	O3-Cu1-N1	94.0(2)	O3-Cu1-O4	98.7(2)
	Cu1-O2^{iv}	2.612	N1-Cu1-O4	104.6(2)		
	Cu1-O3	1.904(5)	O1^{iv}-Cu1-O2	87.3(2)		
	Cu1-O4^{iii}	2.333(6)	O1^{iv}-Cu1-O4^{iii}	90.11(19)		

Symmetry codes: (*i*) -1+*x*, *y*, *z*; (*ii*) 1+*x*, *y*, *z*; (*iii*) +*x*, 1+*y*, *z*; (*iv*) -*x*, -0.5+*y*, 1-*z*.

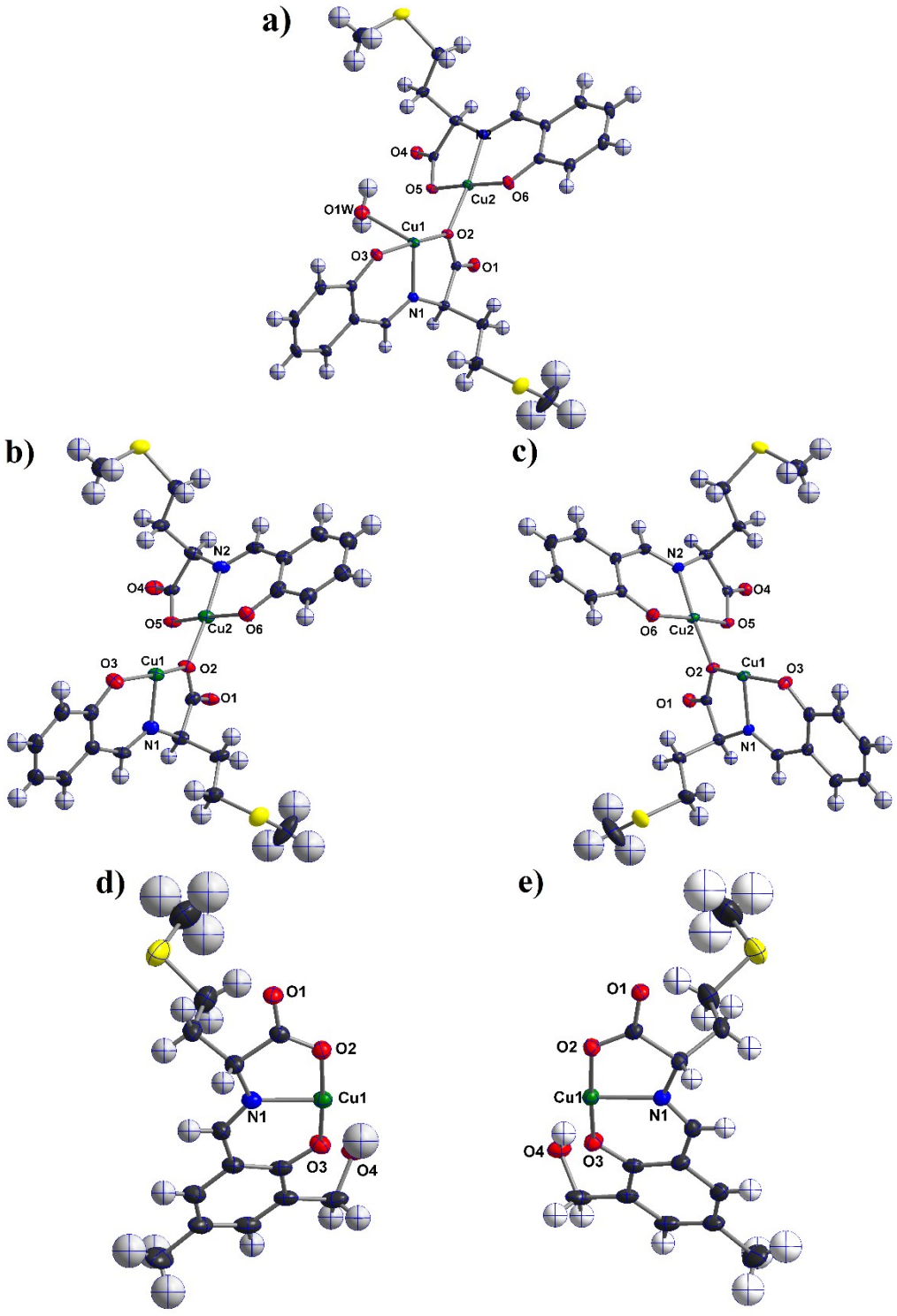

Figure S1. View of the asymmetric unit in **1-*R*·H$_2$O** (a), **1-*R*** (b), **1-*S*** (c), **2-*R*** (d), and **2-*S*** (e) showing 30% probability thermal ellipsoids

Table S2. Continuous Shape Measures (CShMs) for the coordination polyhedron around the Cu(II) ions.

Geometry	Cu1(1-***R***·H_2O)	Cu2(1-***R***·H_2O)
HP-6	32.543	45.426
PPY-6	23.096	**34.001**
OC-6	**2.582**	**34.320**
TPR-6	12.932	**33.335**
JPPY-6	25.734	37.854

Geometry	Cu1(1-***R***)	Cu2(1-***R***)	Cu1(1-***S***)	Cu2(1-***S***)
PP-5	31.024	30.417	30.895	30.499
vOC-5	2.700	2.320	2.512	2.354
TBPY-5	3.309	4.635	3.526	4.695
SPY-5	**2.295**	**1.864**	**2.155**	**1.856**
JTBPY-5	6.946	8.137	6.966	8.345

Geometry	Cu1(2-***R***)	Cu1(2-***S***)
HP-6	37.954	53.588
PPY-6	21.895	39.224
OC-6	**4.612**	**37.285**
TPR-6	12.896	43.186
JPPY-6	26.522	45.070

Geometry	Cu1(3-***R***)	Cu1(3-***S***)
PP-5	31.380	31.508
vOC-5	2.144	2.027
TBPY-5	4.314	4.404
SPY-5	**1.896**	**1.886**
JTBPY-5	7.842	7.657

PP-5_Pentagon; vOC-5_Vacant octahedron; TBPY-5_Trigonal bipyramid; SPY-5_Spherical square pyramid; JTBPY-5_Johnson trigonal bipyramid; HP-6_Hexagon; PPY-6_Pentagonal pyramid; OC-6_Octahedron; TPR-6_Trigonal prism; JPPY-6_Johnson pentagonal pyramid.

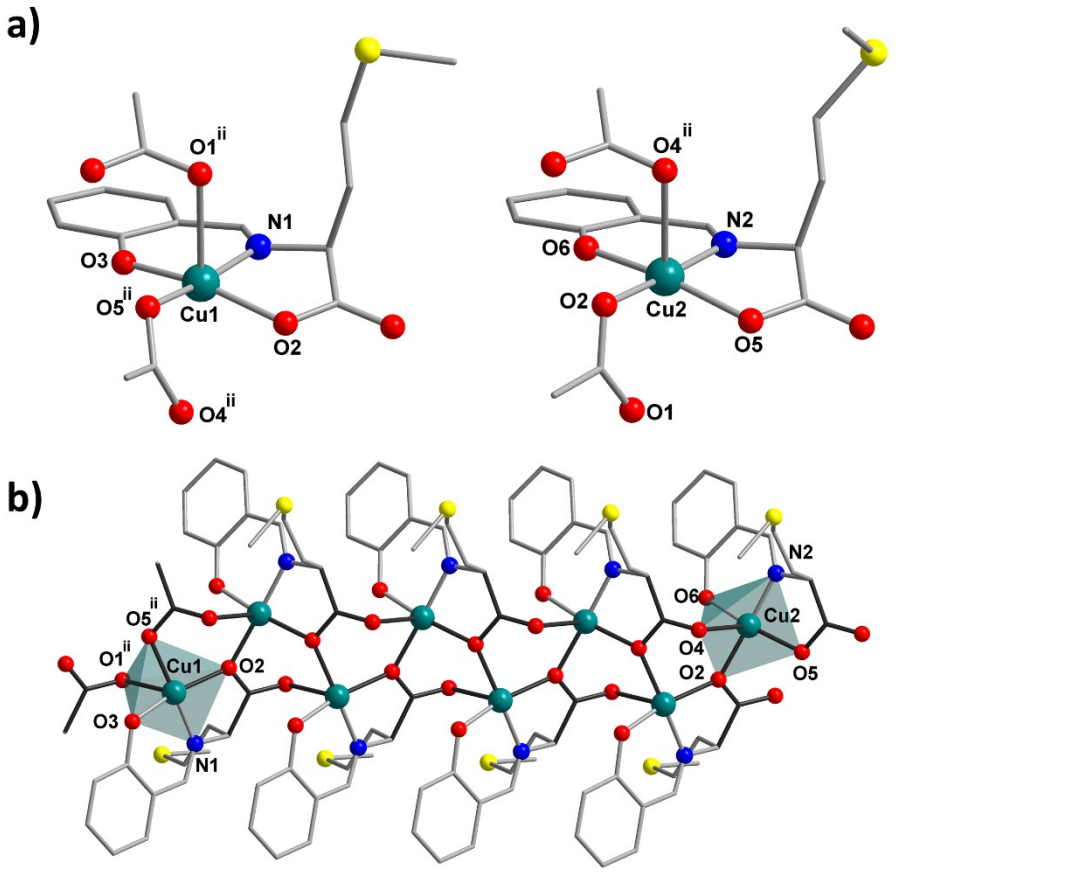

Figure S2. Relevant structural features determined by SC-XRD on **1-*S*** resulting from the single-crystal-to-single-crystal dehydration process: (a) the coordination environment of the two crystallographic independent Cu(II) ions and (b) the helical double chain motif that they construct.

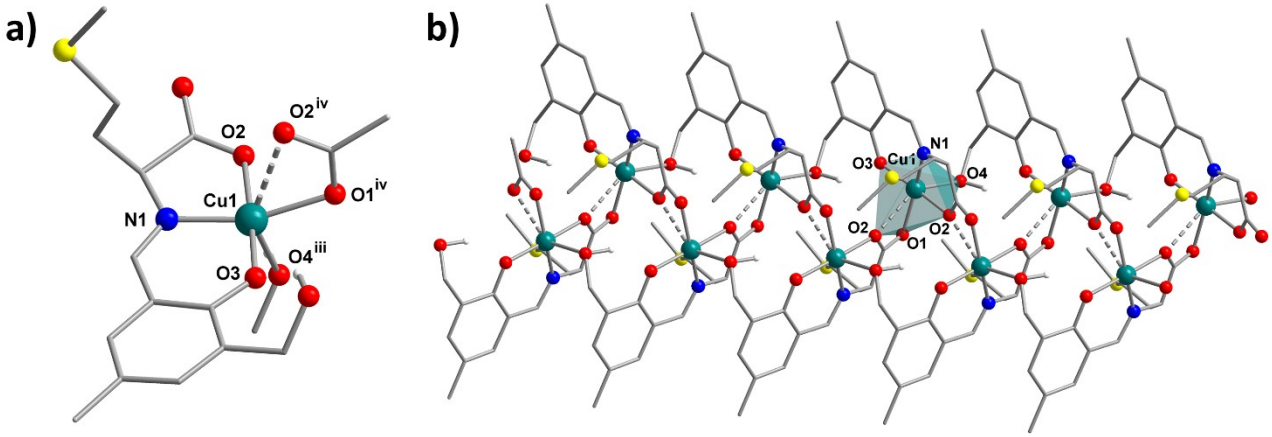

Figure S3. Coordination polyhedron of the copper(II) ion (a) and the resulting helical double chain (b) of **2-*S***.

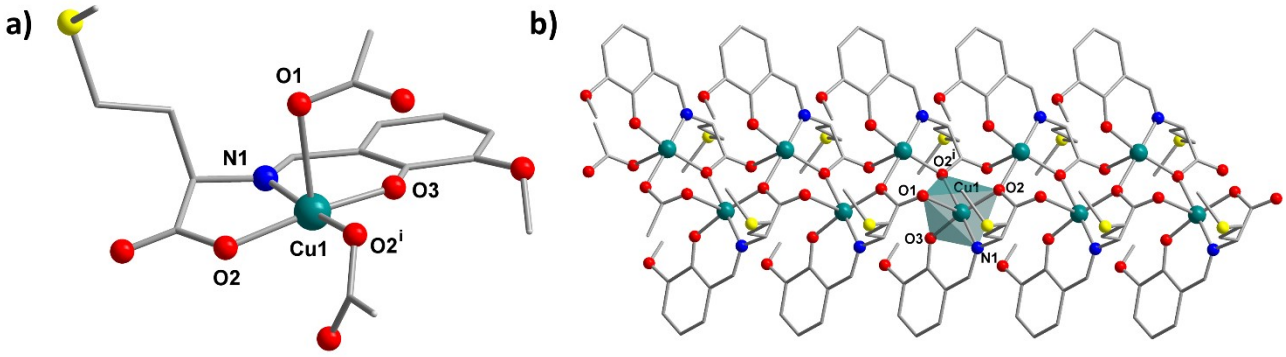

Figure S4. Coordination polyhedron of copper(II) ion (a) and the perspective view of a helical double chain (b) present in the crystal structure of **3-*R*** (for more details and full discussion, see reference C.D. Ene, C. Maxim, M. Rouzières, R. Clérac, N. Avarvari and M. Andruh, *Chem. Eur. J.*, 2018, **24**, 8569-8576).

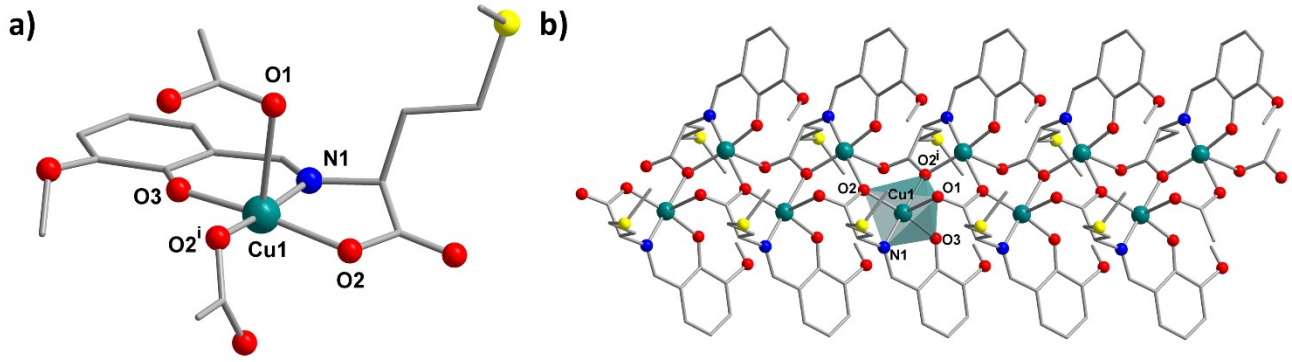

Figure S5. Coordination polyhedron of copper(II) ion (a) and the perspective view of a helical double chain (b) present in the crystal structure of **3-*S*** (for more details and full discussion, see reference C.D. Ene, C. Maxim, M. Rouzières, R. Clérac, N. Avarvari and M. Andruh, *Chem. Eur. J.*, 2018, **24**, 8569-8576).

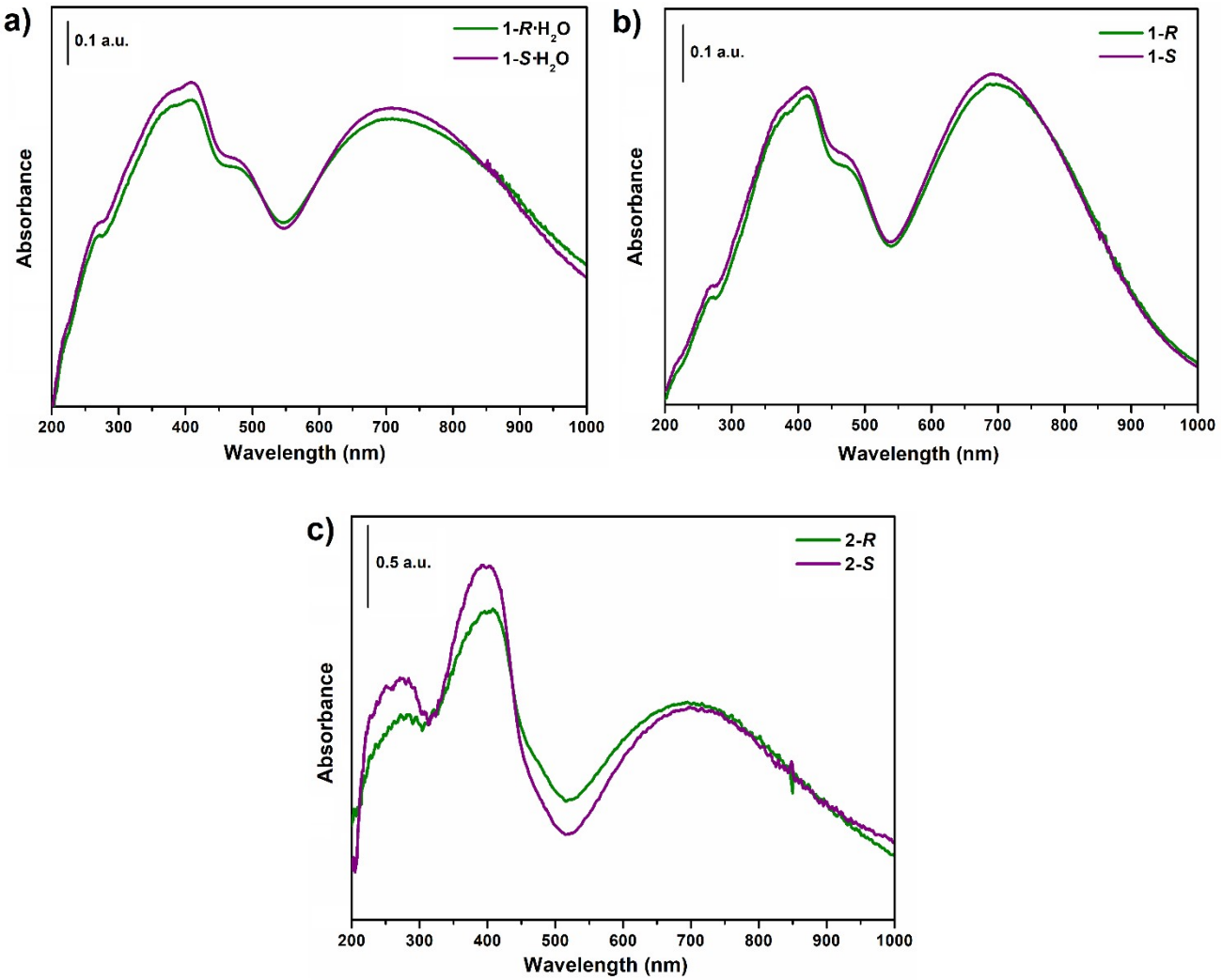

Figure S6. Room temperature diffuse reflectance UV-Vis spectra of the enantiomeric pairs **1-*R*·H$_2$O** and **1-*S*·H$_2$O** (a), **1-*R*** and **1-*S*** (b), **2-*R*** and **2-*S*** (c).

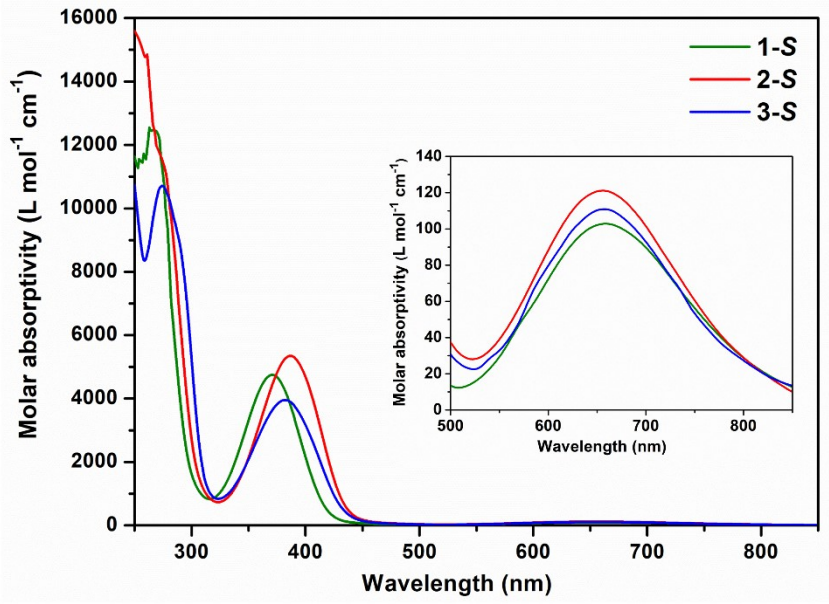

Figure S7. UV-Vis spectra of **1-*S***, **2-*S***, and **3-*S*** in methanol (c = 3.94 x 10^{-4}, 3.46 x 10^{-4}, and 3.57 x 10^{-4} mol·L^{-1}, respectively) recorded at room temperature.

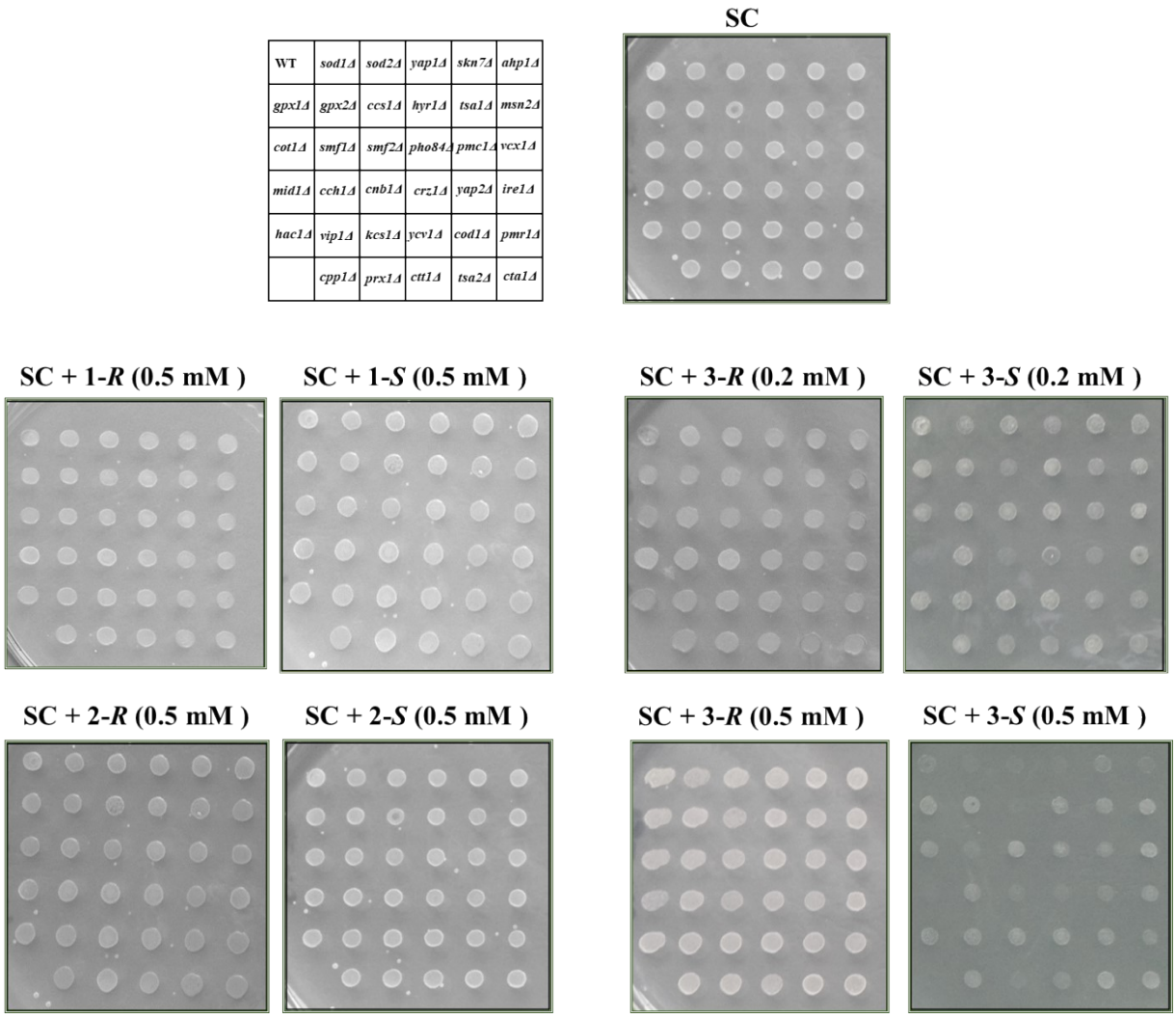

Figure S8. Phenotypic validation screen and confirmation of **3-*S*** selectivity against **1-*R***, **1-*S***, **2-*R***, **2-*S***, **3-*R***. Mid log growing cells (10^6 cells/mL) of the specified strains grown in a 48-well plate were stamped on SC/agar by means of a pin replicator (approximately 5 µL/spot). The agar plates were photographed after 2 days' incubation at 28 °C. Experiments were repeated three times and the results were similar. One representative set is shown.